Performance of a CMOS Bluetooth Transceiver IC with Copper RF Passives

My The Doan, Qian Yin, Khoo Ee Sze, Pradeep B. Khannur, Subhash C. Rustagi, Shi Jinglin, Pang Dow Foo and Aruna B. Ajjikuttira

Institute of Microelectronics, 11 Science Park Rd, Singapore Science Park II, Singapore 117685

Abstract — **On-chip copper inductors, MIM capacitors and precision resistors in a novel, low-cost process are described. A CMOS transceiver for Bluetooth was realized with these new RF passive components and compared with the same IC realized in a commercial 0.35μm CMOS process with Al metalization. In the low-noise amplifier (LNA), a gain improvement of around 5dB and a noise-figure reduction of 1.2dB were observed. For the image-reject mixer (IRM), the conversion gain improved by 3.5dB. The output power of the power amplifier (PA) increased by 1.5dB. For the phase-locked loop (PLL) frequency synthesizer, the settling time was reduced almost in half.**

I. Introduction

Bluetooth ICs using CMOS technology are becoming popular in enabling low-cost, short-range radio links between mobile phones, mobile PCs, and other appliances. We have reported a single-chip transceiver for Bluetooth applications using a commercial 0.35μm CMOS technology [1]. To improve the IC's performance, design margin, and its power consumption, we can either re-design it in a newer generation CMOS technology (such as 0.18μm) or improve on the performance of the RF passive components used such as inductors and metal-insulator-metal (MIM) capacitors. Our near term objective was to improve on the performance of the RF passive components that are integrated on top of a standard 0.35μm CMOS technology. With cost keenly in mind, we designed a novel, low cost process that integrated copper inductors, MIM capacitors and precision resistors with only two additional masking steps. Comparing to other process schemes that are used to integrate the inductor and MIM capacitors [2]-[3], our scheme saves at least one masking step and several associated processing steps. Details of the processing steps will be described in section two. In section three, we show results related to the performance of the RF passive components. The performance of different RF sub-circuits such as LNA, IRM, etc. will be discussed in section four. This will be followed by the conclusion.

II. Process Description and RF Measurements

Our scheme of integrating on-chip planar spiral copper inductor, MIM capacitor and precision resistor is shown in Fig. 1, whilst of others [2]-[3] in Fig. 2. The inductor consists of the top interconnect routing metal level (ca. 0.4μm copper) to which an additional single-damascene thick copper layer (ca. 1.7μm) is coincidentally stacked.

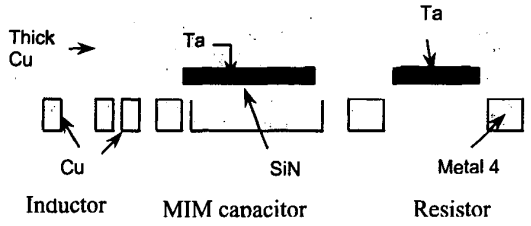

Fig. 1. Schematic device cross-section of a process flow integrating MIM capacitor, inductor, and metal resistor.

The top interconnect copper layer also serves as a low resistance bottom-plate for high-Q MIM capacitors. The standard copper barrier of silicon nitride (SiN) serves as the MIM insulator using a conservative 700Å (ca. 0.9fF/μm^2) to maintain a baseline barrier thickness after capacitor top-plate etch. Tantalum (Ta) serves as the MIM top-plate and is scaled for practical precision metal resistors (ca. 500Å ~ 50 ohm/sq.). Measured results of these passive components are listed in Table 1.

In order to save the expense of a separate through-hole (or "via") masking, as seen in Fig. 2, the Ta top-electrode and resistor ends are directly connected to underlying routing copper using the inductor mask. The features of this inductor mask are relatively non-critical so the oxide step created by the thin Ta layer does not require CMP planarization before lithography. Comparing to other published integration schemes [2]-[3] as shown in Fig. 2, we save at least one via masking step and several associated processing steps (i.e., single-damascene instead of dual-damascene). This keeps cost down.

0-7803-7239-5/02/$10.00 © 2002 IEEE

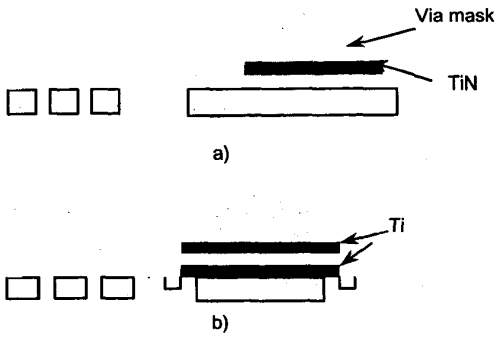

Fig. 2. Schematic device cross-section of published process flows integrating MIM capacitor and Inductor, a) in ref. [3], and b) in ref. [2].

III RF PASSIVE COMPONENT PERFORMANCE

Measured results of the passive components are listed in Table 1.

TABLE 1
SUMMARY OF RF PASSIVES MEASUREMENT

	Q @ 2.5GHz	C/A fF/μm²	Sheet R Ω/sq	TCR ppm/°C
L (2.4nH)	11.2	-	0.09	4150
C (2pF)	65.7	0.9	-	160
R	-	-	53	-100

Comparing to a commercial 0.35μm CMOS process that we had used for our earlier work [1], we leverage on copper's approximately 45% reduction in bulk resistivity over aluminum-alloys to improve the Q-factor. For the MIM capacitor, it was moved up from between metal 2 and metal 3 to metal 4. At the same time, SiN with ε_r value of 7 replaces SiO_2. Theses changes enables higher Q-factor for the MIM capacitors. The leakage current is very low: 5nA/cm² at 10V, and the yield is 100% for 16K um² capacitor. The failure criterion is 1uA/cm² at 6.6V. The Ta precision resistor reduces TCR to -100ppm. Some RF measurement results of our copper inductors and MIM capacitors are shown in Fig. 3 and Fig. 4. Note also that our RF modeling is very accurate for both the inductors and capacitors. This enables us to do circuit optimization by identifying the sources of circuit performance improvement.

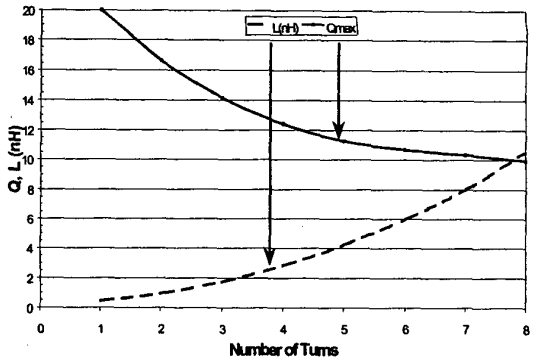

Fig. 3. Inductance and maximum Q-factor of various inductors, width=6μm, spacing=2μm, and hole diameter=75μm.

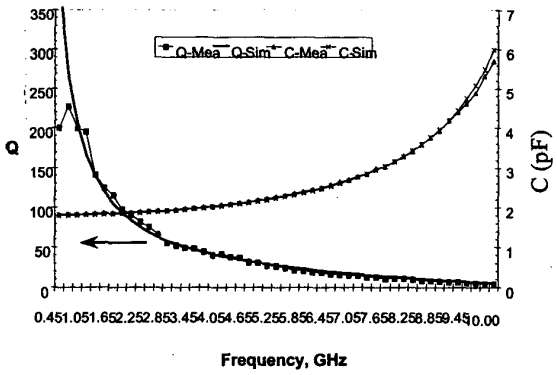

Fig. 4. Measurement vs. simulation of a 2-pF MIM capacitor.

IV. RF CIRCUIT PERFORMANCE

A. Circuit Details and Results

In order to evaluate the performance of the copper RF passives, a CMOS Bluetooth RFIC was chosen as the test vehicle. The inductors and MIM capacitors from the Al Bluetooth RFIC were replaced with the proposed copper RF passives.

Fig. 5 shows the block diagram of the CMOS Bluetooth RFIC [1]. The receiver is based on a single-conversion superheterodyne principle, with an intermediate frequency (IF) of two MHz. The frequency synthesizer is of integer-N PLL type with open-loop modulation. The circuit schematics of the RF blocks making the transceiver IC

may be found in [1]. The IF sections were not modified as they contain no RF passives.

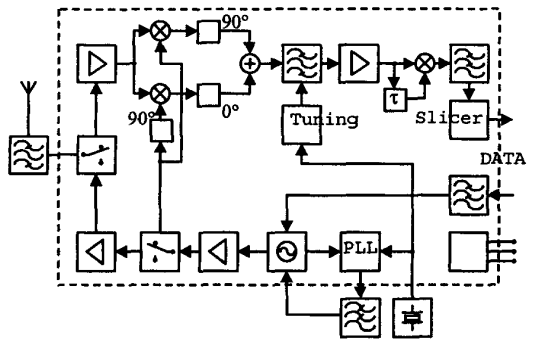

Fig. 5. Block diagram of the transceiver IC.

Low-Noise Amplifier: The LNA serves to amplify the incoming signal. It must add as little noise as possible to the signal that is being amplified. To this end, high Q inductors and capacitors play a critical role. As shown in Fig. 5, the LNA receives single-ended input from the antenna through the transmit-receive (T/R) switch and provides amplified differential signals to the IRM. It consists of two sub-blocks namely the cascode-connected common-source amplifier stage followed by a single-ended to differential converter. The complete circuit uses nine inductors and seven MIM capacitors.

For the LNA with copper passives, the

- gain improved by 5.5 dB from 14.5 dB to 20 dB
- noise-figure improved by 1.2 dB from 5 to 3.8 dB
- supply current increased by 0.7 mA from 9.5 mA to 10.2 mA.

A plot of LNA gain is shown in Fig. 6.

Image-Reject Mixer: The IRM performs the dual function of down-converting the input signal and providing sufficient attenuation to the image signal. The IRM block uses matching networks, Gilbert-cell mixers, poly-phase filters and IF combiner/ amplifier in its implementation. There are a total of 12 inductors and 37 MIM capacitors in the IRM block.

The measurements on the IRM sub-block indicate that:

- the voltage conversion gain improved by 3.5 dB from 24 dB to 27.5 dB
- the image-reject ratio improved by 4 dB from 47 dB to 51 dB
- The Cu IRM is more insensitive to LO power variation compared to the Al version.

A plot of image-rejection ratio is shown in Fig. 7.

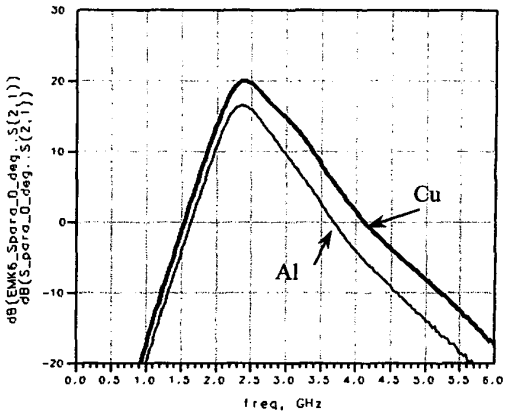

Fig. 6. LNA gain comparison.

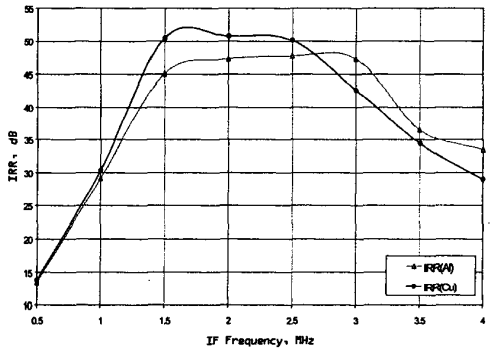

Fig. 7. IRM image-rejection ratio.

Power Amplifier (PA): The PA provides an output of 2.5 dBm for an input signal at -8dBm coming from the VCO. It is a two-stage class-AB circuit with internal feedback to ensure unconditional stability. It uses four inductors and six MIM in its realization.

For the PA, the measurements yield:

- an output power increase of 1.5 dBm
- an increase in supply current of about 0.5 mA from 12.2mA to 12.7mA.

A plot of output power for different on-wafer measurement samples is shown in Fig. 8.

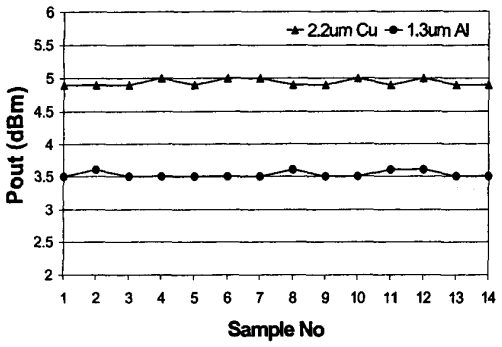

Fig. 8. PA output power, Al vs. Cu.

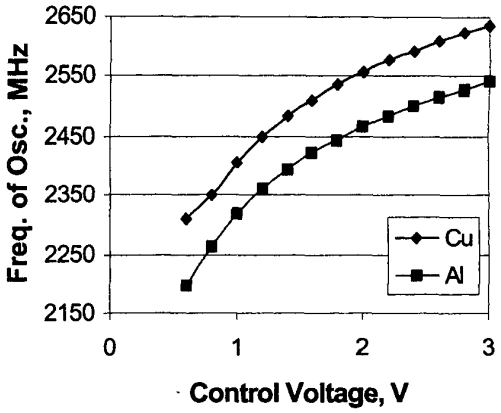

Fig. 9. Tuning curves for Cu and Al VCO.

PLL Synthesizer: The synthesizer covers the ISM band of 2.4 to 2.5 GHz in steps of one MHz. It is designed for frequency-hopping operation. It consists of a PLL, a VCO and the (external) loop filter. The Al inductor in the VCO was replaced with Cu inductor for this evaluation. For the copper VCO, the gain constant at mid-band increased from 115 MHz/V to 195 MHz/V. A plot of the tuning curves is shown in Fig. 9.

For the Cu PLL synthesizer, with the same loop filter, it was observed that:

- the settling-time for a hop from 2.4GHz to 2.5GHz improved from 140μs to 80μs
- the closed-loop phase-noise at 100 kHz offset from a 2450 MHz carrier degraded from -87 dBc/Hz to -81 dBc/Hz.

B. Discussion

In almost all cases the circuit performance improved with copper RF passives. Typically the inductor Q's have increased from about 5 to about 11 and the MIM capacitor area has been reduced in half. For the LNA, the gain and noise-figure improved substantially while the supply current increased a little. For the IRM, the conversion gain and image-reject ratio improved and the sensitivity to LO power variation reduced. In case of the PA, the output power increased while the supply current increased marginally. For the synthesizer, with the same loop filter, the settling time improved substantially while the closed-loop phase-noise at 100 kHz offset degraded by six dB. Both of these are due to the increase in the VCO gain constant.

CONCLUSION

High performance copper inductor, MIM capacitor and precision resistors have been demonstrated on test structures and CMOS RF circuits. The processing steps can be readily integrated into a copper interconnect baseline with minimal modifications. Significant improvements in RF performance were observed even without design optimization for copper behaviour. In the near future RFIC technology, copper as an interconnect metalization is expected and the full advantages of the high quality-factor copper passives can be leveraged.

ACKNOWLEDGEMENT

The authors wish to acknowledge the contributions of Eric Johnson, Mark Hatzilambrou and Chester Leung. They would also like to thank Moe Moe Aung, Oh Boon Hwee and Siao Peck Yong for their assistance.

REFERENCES

[1] A. Ajjikuttira, et al., "A Fully-Integrated CMOS RFIC for Bluetooth Applications", *ISSCC 2001*, pp. 198-189, Feb. 2001.

[2] M. Armacost, et al., "A High Reliability Metal Insulator Metal Capacitor for 0.18 μm Copper Technology", *2000 IEDM Tech. Dig.*, pp. 157-160.

[3] R. Liu, et al., "Single mask metal-insulator-metal (MIM) capacitor with copper damascene metalization for sub-0.18μm mixed mode signal and system on a chip (SOC) applications", *2000 Proc. Int. Interconnect Tech. Conf.*, pp. 111-113.